Comparing observed and modelled components of the Atlantic Meridional Overturning Circulation at 26°N.

Harry Bryden[1], Jordi Beunk[2], Sybren Drijfhout[1,2], Wilco Hazeleger[2], Jennifer Mecking[3]

[1]Ocean and Earth Science, University of Southampton, Southampton United Kingdom
[2]Faculty of Geosciences, University of Utrecht, Utrecht, The Netherlands
[3]National Oceanography Centre, Southampton, United Kingdom

Correspondence Email: hlb@soton.ac.uk

Deleted: Jennifer Mecking[3],
Formatted: Font: Not Bold
Formatted: Font: Times New Roman, 14 pt, Not Bold, Superscript
Formatted: Font: 14 pt

2 February 2024

Deleted: 15 November 2023

Abstract

The Coupled Model Intercomparison Project (CMIP) allows assessment of the representation of the Atlantic Meridional Overturning Circulation (AMOC) in climate models. While CMIP Phase 6 models display a large spread in AMOC strength by a factor of three, the multi-model mean strength agrees reasonably well with observed estimates from RAPID[1], but this does not hold for its various components. In CMIP6 the present-day AMOC is characterised by a lack of lower North Atlantic Deep Water (lNADW), due to the small-scale of Greenland-Iceland-Scotland Ridge overflow and too much mixing. This is compensated by increased recirculation in the subtropical gyre and more Antarctic Bottom Water (AABW). Deep-water circulation is dominated by a distinct deep western boundary current (DWBC) with minor interior recirculation compared to observations. The future decline in the AMOC to 2100 of 7Sv under a SSP5-8.5 scenario is associated with decreased northward western boundary current transport in combination with reduced southward flow of upper North Atlantic Deep Water (uNADW). In CMIP6, wind stress curl decreases with time by 14% so that the wind-driven thermocline recirculation in the subtropical gyre is reduced by 4 Sv (17%) by 2100. The reduction in western boundary current transport of 11Sv is more than the decrease in the wind-driven gyre transport indicating a decrease over time in the component of the Gulf Stream originating in the South Atlantic.

Deleted: sugges

1. Introduction

The Atlantic Meridional Overturning Circulation (AMOC) is the Atlantic part of the global overturning circulation. The global overturning circulation, in which deep waters formed at high latitudes in the northern Atlantic and Weddell Sea flow equatorward, upwell, circulate and eventually flow as upper waters back toward the formation regions, transports heat, freshwater, nutrients and CO_2 throughout the global ocean. The AMOC includes North Atlantic Deep Water (NADW) formation in the subpolar and polar regions of the northern Atlantic, southward flow of NADW in deep western boundary currents, wind-driven circulation in the subtropical and subpolar gyres and northward flow of upper waters notably in the Gulf Stream. Upwelling of NADW occurs principally outside of the North Atlantic. Our understanding of the strength, variability and structure of the AMOC has improved since the deployment of the RAPID[1] array, which monitors the volume transport at 26°N since

[1] RAPID is used here as shorthand for the RAPID-Meridional Overturning Circulation and Heatflux Array-Western Boundary Time Series at 26°N (Moat et al., 2022).

April 2004 (Moat et al., 2020). Additionally, these observations serve as invaluable reference data for the representation of the AMOC in coupled climate and Earth System models. The most recent phase of the Coupled Model Intercomparison Project, CMIP Phase 6, allows us to assess the representation of the AMOC in these models. The models project the AMOC strength will decline over the next century (Lee et al., 2021). Here we compare observed and modeled components of the AMOC over the historical period 2004 to 2014 and then assess how the ensemble-mean CMIP6 transport components change in a declining AMOC over the next century under SSP5-8.5 emission scenario.

The RAPID AMOC observations from 2004 to 2018 indicate that the AMOC has declined by 2.4 Sv, about 12%, from 18.3 Sv to 15.9 Sv (Bryden, 2021). The decline is primarily evident in reduced southward transport of lower North Atlantic Deep Water (lNADW) that is balanced by slightly reduced Gulf Stream transport and more southward recirculation within the subtropical gyre. In CMIP6 models, the AMOC declines by about 40% over the 21st century (Weijer et al., 2020). Here we analyse 19 CMIP6 model projections in order to identify which components lead to the AMOC decline, for clues as to how the AMOC may change within the continuing RAPID observational framework.

The Coupled Model Intercomparison Project (CMIP) is a comprehensive effort of modelling centres around the world to improve our understanding about past, present and future changes of the climate system (Eyring et al., 2016; O'Neill et al., 2016). Even though CMIP6 shows improvements compared to previous CMIP generations, model biases related to the AMOC persist. These include a shallow bias to the deep cell, too much deep convection, and a too-small temperature difference between its upper and lower limbs. Additionally, CMIP6 models largely underestimate low-frequency variability of the AMOC and show large inter-model differences in their AMOC representation (Weijer et al., 2020).

The RAPID array monitors the AMOC volume transport at 26°N since April 2004 (Smeed et al., 2018). The transport through the cross section is estimated by a decomposition of the AMOC into 3 components: (1) transport through the Florida Straits, (2) Ekman surface transport generated by zonal wind stress, and (3) density driven interior transport estimated from mooring measurements. The mid-ocean interior transport is further broken down into thermocline recirculation (0-800m depth)), intermediate water transport (800-1100m), upper North Atlantic Deep Water (1100-3000m), lower North Atlantic Deep Water (3000-5000m). The goal of this study is to gain insight into the cause of disagreement between CMIP6 models and RAPID data in terms of AMOC strength, structure and variability. We decompose the modelled AMOC transport at 26°N from CMIP6 into the same transport components as measured by the RAPID array. We compare the CMIP6 transport components with the observed RAPID components for the historical period 2004-2014. We then examine the change of these components in CMIP6 under the SSP5-8.5 emission scenario from the historical period until 2100.

Deleted: apid

2. Data and Methods

Monthly averages of AMOC estimates from the RAPID array are compared to the historical simulations of 19 CMIP6 models. Note that only the overlapping period was investigated, April 2004 – December 2014. Details of the 19 CMIP6 models are given in Table 1. The SSP5-8.5 future projection from 2015 to 2100, is then used to investigate how the AMOC may change in future projections. For each model, one ensemble member was used as defined in Table 1.

Model	*Modelling centre*	*Horizontal resolution (°)*	*Variant label*	*Data reference historical*	*Data reference SSP585*
CAMS-CSM1-0	CAMS	1 x 1	r1i1p1f1	Rong (2019)	Rong (2019)
CAS-ESM2-0	CAS	1 x 1	r1i1p1f1	Chai (2020)	Unknown (2018)
CESM2-WACCM	NCAR	1 x 1	r1i1p1f1	Danabasoglu (2019)	Danabasoglu (2019)
CIESM	THU	1 x 1	r1i1p1f1	Huang (2019)	Huang (2020)
CMCC-CM2-SR5	CMCC	1 x 1	r1i1p1f1	Lovato and Peano (2020)	Lovato and Peano (2020)
CMCC-ESM2	CMCC	1 x 1	r1i1p1f1	Lovato et al. (2021)	Lovato et al. (2021)
CNRM-CM6-1	CNRM-CERFACS	1 x 1	r1i1p1f2	Voldoire (2019)	Voldoire (2019)
CNRM-ESM2-1	CNRM-CERFACS	1 x 1	r2i1p1f2	Seferian (2018)	-
CanESM5	CCCma	1 x 1	r1i1p1f1	Swart et al. (2019)	Swart et al. (2019)
EC-Earth3	EC-Earth Consortium	1 x 1	r1i1p1f1	EC-Earth Consortium (2021)	EC-Earth Consortium (2019)
FIO-ESM-2-0	FIO-QLNM	1 x 1	r1i1p1f1	Song et al. (2019)	Song et al. (2019)
HadGEM3-GC31-LL	MOHC	1 x 1	r1i1p1f3	Ridley et al. (2019)	Good (2020)
HadGEM3-GC31-MM	MOHC	0.25 x 0.25	r1i1p1f3	Ridley et al. (2019)	Ridley et al. (2019)
IPSL-CM6A-LR	IPSL	1 x 1	r1i1p1f1	Boucher et al. (2021)	Boucher et al. (2019)
MPI-ESM1-2-HR	MPI	0.4 x 0.4	r1i1p1f1	Jungclaus et al. (2019)	Schupfner et al. (2019)
MPI-ESM1-2-LR	MPI	1.5 x 1.5	r1i1p1f1	Wieners et al. (2019)	Wieners et al. (2019)
MRI-ESM2-0	MRI	1 x 0.5	r1i1p1f1	Yukimoto et al. (2019)	Yukimoto et al. (2019)
NESM3	NUIST	1 x 1	r1i1p1f1	Cao and Wang (2019)	Cao (2019)
UKESM1-0-LL	MOHC	1 x 1	r1i1p1f2	Tang et al. (2019)	Good et al. (2019)

Deleted: ¶

Table 1. Metadata and references for the models analysed in this study. The choice of models is motivated by the fact that historical and SSP85 date is available for all used variables including meridional velocity, zonal wind stress, salinity and temperature. In addition only models that use horizontal depth values are included. The choice of ensemble member is indicated and the preferered ensemble member is realisation 1, initialisation 1, physics 1 and forcing 1, indicated by r1i1p1f1. For some models forcing 1 was not available so a different ensemble member was chosen making sure that the forcing version (v6.2.0) is the same. References are from the Earth System Grid Federation.

Deleted: ¶

Deleted: *Table 1: Metadata and references of the models analysed in this stu*

A cross section between Florida and the African continent at the latitude closest to 26°N was selected for each model. The net transport through the section, approximately -1 Sv for each model due to the Bering Strait throughflow, was removed before computing the AMOC components from meridional velocities as follows:

Florida Straits Transport (FS): CMIP6 models do not resolve the Bahama Islands and as a result the Florida Straits proper. For this reason the following definition is used. The boundary between Florida Straits (FS) transport and mid-ocean transport is defined as the longitude where the depth-averaged transport (from the surface down to the depth of maximum overturning) changes from positive (northward) to negative (southward). This definition thus identifies the FS transport as the western boundary current, thereby including the transport by the Antilles Current, which in CMIP6 models cannot be separated from the Florida Current.

For each model, we have made the following choices to define Thermocline Recirculation, Upper North Atlantic Deep Water, Lower North Atlantic Deep Water and Antarctic Bottom Water. The decision was to use potential temperature to determine the boundaries between upper and lower North Atlantic Deep Water in the CMIP6 models. This choice was motivated by the indistinct upper boundary (in depth) of Lower North Atlantic Deep Water in the models.

Thermocline Recirculation (tr): East of FS and from the surface to down to the depth of horizontally averaged potential temperature of 8°C.

Intermediate Waters (iw): East of FS and between the depth of horizontally averaged potential temperature of 8°C and depth of maximum overturning.

Upper North Atlantic Deep Water (uNADW): Between the depth of maximum overturning and the depth of horizontally averaged potential temperature of 3°C.

Lower North Atlantic Deep Water (lNADW): Between the depth of horizontally averaged potential temperature of 3°C and the depth where horizontally-averaged transport changes from negative to positive.

Antarctic Bottom Water (AABW): Between the depth where horizontally-averaged transport changes from negative to positive and the bottom.

Ekman (ek): Near surface ageostrophic transport estimated from the zonal wind stress.

Multi-model means (MMM) for each component over the 19 models are then made with their standard deviation.

3. Results

Figure 1 compares the RAPID observations of the AMOC transport components with the CMIP6 components for the historical period 2004-2014. For the historical period (2004-2014) the MMM CMIP6 AMOC underestimates the observed AMOC transport by 2.2 Sv (Table 2). The underestimation of AMOC strength in the CMIP6 models is likely related to the reduced transport of lower NADW, due to the small scale of Greenland-Iceland-Scotland Ridge overflow compared to the resolution of models and excessive mixing at this location. In a study of deep waters in CMIP6, Heuzé (2021) noted that the models did form water masses similar in properties to lNADW in the Nordic Seas, but none of the deep waters made it over the ridge and into the Iceland or Irminger basins. In the models, this lack of lNADW is partially compensated by increased southward flow of upper NADW so the total southward flow of deep water in CMIP6 is comparable to that observed by RAPID. The variability of NADW is underestimated, most likely due to the inability of models to reproduce lower NADW overflow. Deep-water circulation in models is dominated by a distinct DWBC with minor interior recirculation compared with observations. CMIP6 MMM Florida Straits (FS) transport (37.4 Sv) is larger than observed Florida Straits transport (31.3 Sv). The relatively coarse-resolution models do not resolve the narrow Florida Straits, and the model western boundary current includes the narrow Antilles Current east of the Bahamas as well as the Gulf Stream flow through Florida Straits. The Antilles Current has maximum northward velocity at 360m depth and the core of the Current is within 50 km of the Bahama Islands. Recent estimates of Antilles Current transport are about 5 Sv (Meinen et al., 2019) and adding this transport to the observed Florida Straits transport suggests that the observed (36.3 Sv) and modeled (37.4 Sv) western boundary current transports are similar. The low-frequency variability of Florida Straits transport is largely overestimated in CMIP6 models and we hypothesize that the inclusion of the Antilles Current in this component in models may be a significant contributor to this variability as the observed Antilles Current transport exhibits rms variability of 7.5 Sv that is not correlated with Florida Straits transport variability. The MMM thermocline recirculation (tr) in CMIP6 models (-26.2 Sv) is larger than observed by the RAPID array (-18.6 Sv) though again this may be due to issues on how the Antilles Current transport is accounted in the observations and in the models. RAPID estimates

Deleted: 10

thermocline recirculation to be the overall southward flow above 800m depth between the Bahamas and Africa and this overall flow includes both the Antilles Current transport and the mid-ocean thermocline recirculation associated with the wind-driven subtropical gyre. If we separate out the northward Antilles Current transport of 5 Sv, then the mid-ocean thermocline recirculation for RAPID would be -23.6 Sv (Table 2) in more reasonable agreement with the CMIP6 MMM thermocline circulation of -26.2 Sv. Overall, the MMM circulation in CMIP6 models for the historical period reasonably represents the observed circulation in RAPID except for the underestimated lNADW transport associated with issues of model representation of flows over ridges.

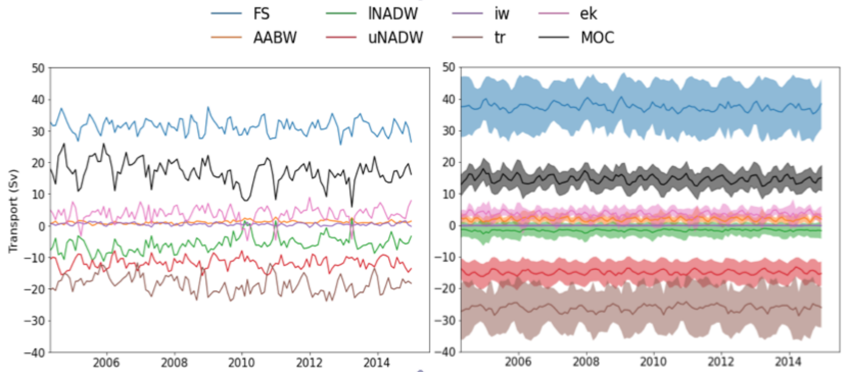

Figure 1. Historical time series for RAPID data (left) and multi-model mean CMIP6 data (right). Shaded areas indicate one standard deviation of the ensemble spread.

		CMIP6 Average		
	Rapid (2004-14)	Historical (2004-14)	2090-2100	Decline
Upper Water				
Florida Straits (FS)	31.3			
Ekman	3.6	3.5	3.4	0.1 (1%)
Intermediate Water (IW)	0.4	----	----	
Thermocline Recirculation (TR)	-18.6			
AMOC=FS+Ekman+IW+TR	16.7			
Antilles Current (AC)	5			
Western Boundary Current (FS+AC)	36.3	37.4	26.4	11 (30%)
Thermocline Recirculation +AC	-23.6			
Model Thermocline Recirculation		-26.2	-21.8	4.4 (17%)
Western Boundary Current+Ekman+Model TR		14.7	8.0	6.7 (45%)
Deep Water				
uNADW	-11.9	-14.9	-9.9	5.0 (34%)
lNADW	-5.9	-1.6	-0.2	1.4 (85%)
AABW	1.0	1.9	2.1	-0.2 (9%)
AMOC=uNADW+lNADW+AABW	-16.8	-14.6	-8.0	6.6 (45%)

Table 2. Components of the Atlantic Meridional Overturning Circulation at 26°N. Model western boundary current includes both Florida Straits and Antilles Current transports. The observed Antilles Currrent (AC) transport of 5 Sv is a rounded value from Meinen et al. (2019)'s mean transport of 4.7±7.5 Sv. For standard RAPID analyses, thermocline recirculation includes Antilles Current transport.

Deleted: This is Figure 6 in Beunk (2022)

Table 2. Components of the Atlantic Meridional O

	Rapid (2004-14)
Upper Water	
Florida Straits (FS)	31.3
Ekman	3.6
Intermediate Water (IW)	0.4
Thermocline Recirculation (TR)	-18.6
AMOC=FS+Ekman+IW+TR	16.7
Antilles Current (AC)	5
Western Boundary Current (FS+AC)	36.3
Thermocline Recirculation +AC	-23.6
Model Thermocline Recirculation	
Western Boundary Current+Ekman+Model TR	
Deep Water	
uNADW	-11.9
lNADW	-5.9
AABW	1.0
AMOC=uNADW+lNADW+AABW	-16.8

CMIP6 model projections suggest that the AMOC will decline over the next century as noted by Weijer et al. (2020). Here we find that the AMOC declines by 45% over the period 2015 to 2100 in a MMM of 19 CMIP6 projections. For comparison, over the RAPID time period 2004 to 2021, the AMOC has exhibited a small (order 12%) reduction that is manifest principally in reduced southward transport of lNADW (Bryden, 2021). It is of interest to identify which components contribute to the projected 45% decline in the AMOC over the coming century in CMIP6 simulations.

All 19 CMIP6 models analysed here exhibit a decline in the AMOC over the 21st century (Table 3). This decline of the AMOC under SSP5-8.5 is in line with other modelling studies (Levang and Schmitt, 2020; Weijer et al, 2020; Roberts et al., 2020). Averaged over the 19 models, the AMOC decline from 2004-2014 to 2090-2100 is 6.6 Sv or 45% in the AMOC transport for the historical period (Figure 2). We find that the decline in the AMOC at 26°N in CMIP6 models from 2015 to 2100 is dominated by a 30% decrease in western boundary current transport (FS in Figure 2) and a 34% reduction in southward deep water transport (uNADW in Figure 2). As Ekman transport (ek) shows no significant change in the model projections, the AMOC decline of 6.6 Sv in the upper waters is the result of the difference between the decline in western boundary current (FS) transport of 11.0 Sv and the 17% decline in southward thermocline recirculation (tr) of 4.4 Sv. For the lower waters the overall decline in northward transport of upper waters of 6.6 Sv is compensated by a decrease in uNADW transport of 6.4 Sv and a small increase in northward AABW transport of 0.2 Sv, so that the net transport through the cross section remains zero.

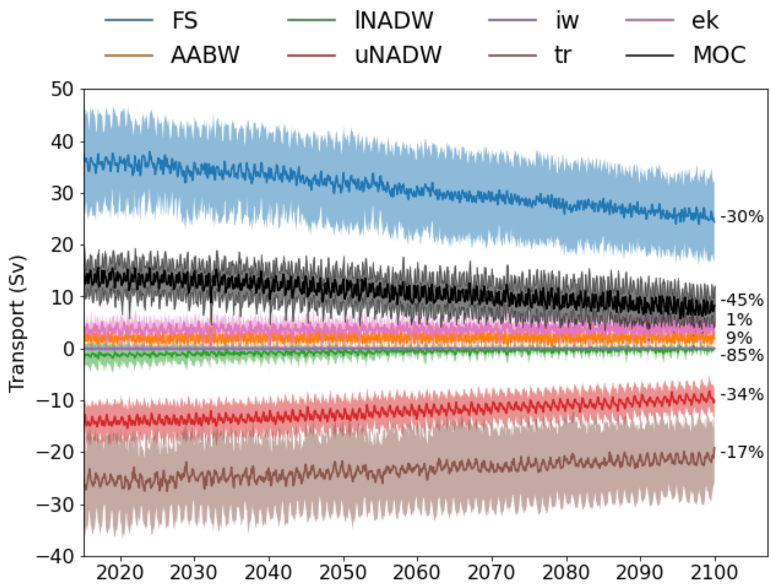

Figure 2. Multi-model mean timeseries of each component under SSP5-8.5. Shaded areas illustrate one standard deviation of the inter-model spread. Percentages show the decline relative to the historical period.

Deleted: 5

Deleted: This is Figure 12 In Beunk (2022).

Model name	Historical mean (Sv)	2090-2100 mean (Sv)	Change (Sv)	Change (%)
CAMS-CSM1-0	12.4	8.9	-3.5	-28
CAS-ESM2-0	18.4	13.7	-4.7	-26
CESM2-WACCM	17.9	6.8	-11.1	-62
CIESM	11.4	4	-7.4	-65
CMCC-CM2-SR5	14.2	9.2	-5.0	-35
CMCC-ESM2	13.3	9.3	-4.0	-30
CNRM-CM6-1	15.7	6.9	-8.8	-56
CNRM-ESM2-1	15.3			
CanESM5	11.4	5.5	-5.9	-52
EC-Earth3	16.2	10.7	-5.5	-34
FIO-ESM-2-0	17.7	10.7	-7.0	-39
HadGEM3-GC31-LL	15.2	7.9	-7.3	-48
HadGEM3-GC31-MM	15.4	6.5	-8.9	-58
IPSL-CM6A-LR	11.6	6.5	-5.1	-44
MPI-ESM1-2-HR	14.8	8.6	-6.2	-42
MPI-ESM1-2-LR	16.6	11.4	-5.2	-31
MRI-ESM2-0	15.4	5	-10.4	-67
NESM3	9.0	5	-4.0	-45
UKESM1-0-LL	15.6	7.8	-7.8	-50

Table 3. Values of the total AMOC for every model. Shown are the historical mean values, 2090-2100 mean values, absolute change and relative change. Changes are relative to the historical period.

To examine changes in wind-driven circulation over the 21st century in the subtropical North Atlantic, we examined the mean wind-stress curl along the 26°N section for the historical and SSP5-8.5 period. The values are negative (i.e. clockwise rotation), which results in southward mid-ocean Sverdrup transport. Since the upper level gyre circulation is driven by wind-stress curl (DiNezio et al., 2009; Zhao and Johns, 2014), we expect a decrease of this driver to affect both Florida Straits transport and thermocline recirculation. Averaged over the model projections, wind stress curl decreases by 14% from about 6 x 10^{-8}m s^{-2}. On the basis of Sverdrup dynamics, we expect this change in wind stress curl will reduce the thermocline recirculation at 26°N and indeed the thermocline recirculation does decrease by 4.4 Sv or 17% over the 21st century. We conclude that the reduction of thermocline recirculation is almost entirely caused by a decline in wind-stress curl and the decline in the directly wind-driven component of the AMOC is exactly reflected in the 17% decline of the Thermocline Recirculation (tr in Figure 2). On the basis of western intensification theory (Stommel, 1948), the decrease in wind-stress curl should also lead to a decrease in western boundary current transport by a similar amount. Thus we can explain a decrease in western boundary current transport of 4.4 Sv over the 21st century as being due to changes in the wind forcing.

The change in the western boundary current transport of 11 Sv in the CMIP projections is due to a reduction in the wind-driven component by 4.4 Sv and to a reduction in the component of the Gulf Stream flow originating from the South Atlantic of 6.6 Sv. The overall 6.6 Sv reduction in the northward flow in the upper waters is then compensated by a reduction in southward flow of the deep waters. In CMIP6, the reduction in the southward flow of deep water is almost entirely due to a decreased DWBC transport of uNADW over the period 2015-2100. Hence the decline in the thermohaline component is reflected in the 34% decline in uNADW transport (uNADW in Figure 2). Overall, the projected AMOC reduction over the 21st century in CMIP6 is due to a reduction in the thermohaline circulation where there is less northward transport of upper waters principally in the western boundary current across 26°N

Deleted: r

Deleted: i

Deleted: This Table is Appendix G in Beunk (2022).

Deleted: Thus

and less southward deep water transport in the deep western boundary current.

4. Discussion

There is much interest in whether the AMOC will decline over the 21st century. Recent analyses of historical observations using Bayesian methods have concluded that the Gulf Stream has weakened by about 1 Sv over the past 40 years (Piecuch and Beal, 2023) and that the AMOC will decline markedly over the next 50 years (Ditlevsen and Ditlevsen, 2023). These studies have generated great media interest. Here we use CMIP6 forward model projections under expected climate forcing (SSP5-8.5) to assess what state-of-the-art coupled climate models 'predict' for the AMOC over the 21st century. McCarthy and Caesar (2023) have argued that models like CMIP6 have not been able to simulate large AMOC variations in the paleo record and hence should not be relied upon to generate accurate projections of future AMOC. Comparisons between model projections and observed circulation variability like those presented above do provide an assessment of the models ability to reliably project the future course of the AMOC. CMIP6 models project declines in both wind-driven and thermohaline components of the AMOC out to 2100. Comparing these projections with ongoing observations like RAPID then provides a reality check on the ability of present models to define future climate change.

Over the SSP5-8.5 period (2015-2100) in CMIP6 projections, we find declines in the western boundary current transport, thermocline recirculation and NADW transport. Decreased thermocline recirculation is related to a decline in wind stress curl along the section and this decline is also expected to contribute to the decline in Gulf Stream transport. But the decline in western boundary current transport in CMIP6 models is substantially greater than the decline in wind stress curl and accompanying thermocline recirculation. Therefore, for the upper water circulation the CMIP6 decline in the AMOC is mostly caused by a decrease in the component of the western boundary current associated with the thermohaline circulation. For the lower water circulation, the decline in southward transport over the SSP5-8.5 period is associated with reduced uNADW transport. The overall reduction in southward deep water transport suggests a decline in NADW formation.

In a similar study, Asbjornsen and Arthun (2023) examined future changes in the AMOC using 14 CMIP6 models and found a weakening AMOC by 8.5 Sv over the coming century. For their ensemble, the Gulf Stream weakened by 33% or 11.2 Sv, 3.7 Sv of which was due to change in wind stress, and the Deep Western Boundary Current transport weakened by 8.5 Sv. As noted above, the CMIP6 projections are consistent in projecting a decline in the AMOC this century (Table 3), but the exact size of the AMOC reduction depends on which models are used for the study.

Because the AMOC is responsible for most of the northward heat transport in the Atlantic Ocean (Johns et al., 2011; Johns et al., 2023), CMIP6 model projections also exhibit a decrease in northward heat transport at 26°N over the 2015-2100 time period (Mecking and Drijfhout, 2023). The northward ocean heat transport across 26°N decreases by an average of 0.3 PW for the SSP5-8.5 scenario and this represents a 30% decline from the historical value of 1.0 PW.

The decline in the thermohaline circulation at 26°N implies that the overturning circulation south of 26°N, that is in the global circulation outside the North Atlantic, has also changed.

The extra-Atlantic circulation converts deep water into upper and intermediate waters so that the southward deep water flow across 26°N and out of the North Atlantic must ultimately be converted within the global ocean into upper and intermediate waters that flow back into the North Atlantic and northward across 26°N. The decline in the North Atlantic thermohaline circulation at 26°N suggests that this global-scale overturning circulation must also have changed. Baker et al (2023) have explored how 2 mechanisms converting deep water into upper water south of 26°N change within CMIP6 simulations. The 2 mechanisms considered are Southern Ocean upwelling associated with eastward wind stress around Antarctica (Toggweiler and Samuels, 1993) and Indo-Pacific diffusive upwelling associated with deep interior mixing (Munk, 1966). Baker et al. found that the wind stress around Antarctica did not decline enough to account for a reduced 6 Sv upwelling of deep water, in fact there appeared to be a small increase in Southern Ocean wind stress and upwelling. Instead they found evidence in the CMIP6 projections that the interior Indo-Pacific upwelling declined enough to account for reduced conversion of deep waters into thermocline waters. They attributed such decline to the global warming that increases stratification (Li et al., 2020) and inhibits vertical mixing and associated upwelling.

Overall, the Atlantic and global overturning circulations appear to have declined in CMIP6 projections from 2015 to 2100. The manifestation of these declines at 26°N include a reduction in the southward transport of NADW and a compensating reduction in the northward flow of upper and thermocline waters through Florida Straits. The reduction in southward deep water transport in CMIP6 is linked to a lack of lNADW formed in the Nordic Seas flowing out over the Greenland-Iceland-Scotland Ridge into the northern Atlantic (Heuzé, 2021); and the reduction in northward flow of upper waters is linked to a decrease in diffusive upwelling in the Indo-Pacific related to increased stratification due to global warming (Li et al., 2020; Baker et al., 2023). The ability of coupled climate models to realistically include these critical processes of deep water formation, mixing in ridge overflows and mid-ocean diffusive upwelling for future projections of ocean circulation should be carefully assessed. In particular, the representation of deep water formation in coupled climate models could be examined in comparison with observed production of deep water. Implementing mixing parameterisations for overflows (Holt et al., 2017) in coupled climate models could be assessed for their effectiveness in allowing the southward transport of lNADW into and through the North Atlantic. And coupled climate models could be examined for their parameterisations of diffusive mixing and upwelling, testing how different parameterisations affect the global ocean overturning circulation over century time scales.

In terms of observations, our results suggest that the ongoing RAPID project should separately measure the Antilles Current and add it to Florida Straits transport for a true measure of western boundary current transport for comparison with modelled transport components. And the Antilles Current transport should be separated from the net mid-ocean southward flow across 26N in the upper 800m that RAPID labels thermocline recirculation so as to identify the actual mid-ocean thermocline recirculation associated with the wind stress curl. By separately estimating the Antilles Current transport contribution, the RAPID project could then provide well-defined estimates for the wind-driven and thermohaline contributions to the AMOC at 26°N.

Code Availability

The code used to obtain the results of this study and a file containing metadata of the models is freely available on GitHub: https://github.com/jordibeunk/MSc_Thesis.git

Data Availability

RAPID data and notes are freely available at https://rapid.ac.uk/rapidmoc/rapid_data/datadl.php

19 CMIP6 models are used. CMIP6 data was accessed and analysed using the super-data-cluster JASMIN (Lawerence et al. 2013). The choice of these models is motivated by the fact that both historical (2004-2015) data and future (2015-2100) projections under Shared Socioeconomic Pathway 5-8.5 are available for all used variables. The model data has been accessed through the Centre for Environmental Data Analysis (CEDA) archive https://data.ceda.ac.uk

Author Contributions

This work is based on an MSc thesis by Jordi Beunk at Utrecht University. Jennifer Mecking, Sybren Drijfhout and Harry Bryden designed the Masters project. Sybren Drijfhout and Wilco Hazeleger identified the student and supervised the project in Utrecht while Mecking and Bryden provided advice during the project and write-up of the thesis. After finishing the thesis, Jordi Beunk initially indicated that he did not wish to write up the results for publication. Harry Bryden prepared a draft for this paper based on Beunk's thesis. Drijfhout, Hazeleger and Mecking then edited the draft and all authors added elements of discussion related to recent papers based on CMIP6 results. Beunk at a late stage indicated he would like to participate in publishing this work and all authors contributed to revising the work in response to Referee comments.

Competing interests

The contact author declares that none of the authors has any competing interests

Acknowledgments

UK Natural Environment Research Council, US National Science Foundation and US National Oceanic and Atmospheric Administration provide funding for the RAPID project and make the data freely available. We acknowledge the World Climate Research Programme, which, through its Working Group on Coupled Modelling, coordinated and promoted CMIP6. We thank the climate modelling groups for producing and making available their model output, the Earth System Grid Federation (ESGF) for archiving the data and providing access, and the multiple funding agencies who support CMIP6 and ESGF. Bryden was a lead investigator for the NERC-funded project that first deployed the transocean Rapid instrument array in 2004 under grant NER/T/S/2002/00481 and he has continued to carry out analyses involving the ongoing Rapid observations following formal retirement in 2011. Drijfhout and Mecking have been funded by NERC under the Wider Impacts of Subpolar North Atlantic decadal variability on the ocean and atmosphere (WISHBONE) grant NE/T0133478/1.

References

Asbjørnsen, H. and Årthun, M.: Deconstructing future AMOC decline at 26.5 N, Geophys. Res. Lett.,

Formatted: Font: (Default) Times New Roman, 12 pt

Deleted: CMIP6 data was accessed and analysed using the super-data-cluster JASMIN (Lawerence et al. 2013).

Formatted: Font: (Default) Times New Roman

Formatted: Font: (Default) Times New Roman, 12 pt

Formatted: Font: Times New Roman

Deleted: 0

Deleted: be involved in

Deleted: ing

Deleted: Mecking and

Deleted: We acknowledge the World Climate Research Programme, which, through its Working Group on Coupled Modelling, coordinated and promoted CMIP6. We thank the climate modelling groups for producing and making available their model output, the Earth System Grid Federation (ESGF) for archiving the data and providing access, and the multiple funding agencies who support CMIP6 and ESGF.

Deleted: Asbjørnsen, H. and Årthun, M., 2023. Deconstructing future AMOC decline at 26.5 N. Geophysical Research Letters, 50(14), p.e2023GL103515

Baker, J. S., Bell, M. J., Jackson, L. C., Renshaw, R., Vallis, G. K., Watson, A. J. & Wood, R. A. (2023). Overturning pathways control AMOC weakening in CMIP6 Models. Geophysical Research Letters, 50, e2023GL.103381. https://doi.org/10.1029/2023GL.103381

Beunk, Jordi (2022). Comparing observed and modeled decomposition of the Atlantic Meridional Overturning Circulation at 26°N. MSc Thesis, Department of Geosciences, Utrecht University, 54p.

Boucher, Olivier; Denvil, Sébastien; Levavasseur, Guillaume; Cozic, Anne; Caubel, Arnaud; Foujols, Marie-Alice; Meurdesoif, Yann; Balkanski, Yves; Checa-Garcia, Ramiro; Hauglustaine, Didier; Bekki, Slimane; Marchand, Marion (2021). IPSL IPSL-CM6A-LR-INCA model output prepared for CMIP6 CMIP historical. Version 20211003.Earth System Grid Federation. https://doi.org/10.22033/ESGF/CMIP6.13601

Boucher, Olivier; Denvil, Sébastien; Levavasseur, Guillaume; Cozic, Anne; Caubel, Arnaud; Foujols, Marie-Alice; Meurdesoif, Yann; Cadule, Patricia; Devilliers, Marion; Dupont, Eliott; Lurton, Thibaut (2019). IPSL IPSL-CM6A-LR model output prepared for CMIP6 ScenarioMIP ssp585. Version 20211003.Earth System Grid Federation. https://doi.org/10.22033/ESGF/CMIP6.5271

Bryden, H. L. (2021). Wind-driven and buoyancy-driven circulation in the subtropical North Atlantic Ocean. *Proceedings of the Royal Society A*, *477*(2256), 20210172.

Buckley, M. W., & Marshall, J. (2016). Observations, inferences, and mechanisms of the Atlantic Meridional Overturning Circulation: A review. *Reviews of Geophysics*, *54*(1), 5-63.

... [1]

50, e2023GL.103515, https://doi.org/10.1029/2013GL.103515, 2023.

Baker, J. S., Bell, M. J., Jackson, L. C., Renshaw, R., Vallis, G. K., Watson, A. J. and Wood, R. A.: Overturning pathways control AMOC weakening in CMIP6 Models, Geophys. Res. Lett., 50, e2023GL.103381, https://doi.org/10.1029/2023GL.103381, 2023.

Beunk, J.: Comparing observed and modeled decomposition of the Atlantic Meridional Overturning Circulation at 26°N, MSc Thesis, Department of Geosciences, Utrecht University, 54p, 2022.

Boucher, O., Denvil, S., Levavasseur, G., Cozic, A., Caubel, A., Foujols, M.-A., Meurdesoif, Y., Balkanski, Y., Checa-Garcia, R., Hauglustaine, D., Bekki, S., and Marchand, M.: IPSL IPSL-CM6A-LR-INCA model output prepared for CMIP6 CMIP Historical, Version 20211003, Earth System Grid Federation, https://doi.org/10.22033/ESGF/CMIP6.13601, 2021.

Boucher, O., Denvil, S., Levavasseur, G., Cozic, A., Caubel, A., Foujols, M.-A., Meurdesoif, Y., Cadule, P., Devilliers, M., Dupont, E., and Lurton, T.: IPSL IPSL-CM6A-LR model output prepared for CMIP6 Scenario MIP ssp585, Version 20211003, Earth System Grid Federation, https://doi.org/10.22033/ESGF/CMIP6.5271, 2019.

Bryden, H. L.: Wind-driven and buoyancy-driven circulation in the subtropical North Atlantic Ocean, Proc. Roy. Soc. A, *477*(2256), 20210172, https://doi.org/10.1098/rspa.2021.0172, 2021.

Buckley, M. W., and Marshall, J.: Observations, inferences, and mechanisms of the Atlantic Meridional Overturning Circulation: A review, *Rev. Geophys.*, *54*(1), 5-63, https://doi.org/10.1002/2015RG000493, 2016.

Cao, J.: NUIST NESMv3 model output prepared for CMIP6 ScenarioMIP ssp585, Version 20211003, Earth System Grid Federation. https://doi.org/10.22033/ESGF/CMIP6.8790, 2019.

Cao, J, and Wang, B.: NUIST NESMv3 model output prepared for CMIP6 CMIP historical, Version 20211003, Earth System Grid Federation, https://doi.org/10.22033/ESGF/CMIP6.8769, 2019.

Chai, Z.: CAS CAS-ESM1.0 model output prepared for CMIP6 CMIP historical, Version 20211003,Earth System Grid Federation, https://doi.org/10.22033/ESGF/CMIP6.3353, 2020.

Unknown: CAS CAS-ESM1.0 model output prepared for CMIP6 ScenarioMIP ssp585, Earth System Grid Federation, http://cera-www.dkrz.de/WDCC/meta/CMIP6/CMIP6.ScenarioMIP.CAS.CAS-ESM2-0.ssp585, 2018.

Danabasoglu, G.: NCAR CESM2-WACCM model output prepared for CMIP6 ScenarioMIP ssp585, Version 20211003, Earth System Grid Federation, https://doi.org/10.22033/ESGF/CMIP6.10115, 2019.

Danabasoglu, G.: NCAR CESM2-WACCM-FV2 model output prepared for CMIP6 CMIP Historical, Version 20211003, Earth System Grid Federation. https://doi.org/10.22033/ESGF/CMIP6.11298, 2019.

DiNezio, P. N., Gramer, L. J., Johns, W. E., Meinen, C. S., and Baringer, M. O.: Observed interannual variability of the Florida Current: Wind forcing and the North Atlantic Oscillation. J. Phys. Oceanogr., 39(3), 721-736, 2009.

Ditlevsen, P., and Ditlevsen, S.: Warning of a forthcoming collapse of the Atlantic meridional overturning circulation, Nature Comm., 14:4254, https://doi.org/10.1038/s41467-023-39810-w, 2023.

EC-Earth Consortium (EC-Earth): EC-Earth-Consortium EC-Earth3 model output prepared for CMIP6 ScenarioMIP ssp585, Version 20211003, Earth System Grid Federation. https://doi.org/10.22033/ESGF/CMIP6.4912, 2019.

EC-Earth Consortium (EC-Earth): EC-Earth-Consortium EC-Earth-3-CC model output prepared for CMIP6 CMIP historical, Version 20211003, Earth System Grid Federation, https://doi.org/10.22033/ESGF/CMIP6.4702, 2021.

Eyring, V., Bony, S., Meehl, G. A., Senior, C. A., Stevens, B., Stouffer, R. J., and Taylor, K. E.: Overview of the Coupled Model Intercomparison Project Phase 6 (CMIP6) experimental design and organization, Geoscientific Model Development, *9*(LLNL-JRNL-736881), 1937–1958, https://doi.org/10.5194/gmd-9-1937-2016, 2016.

Good, P.: MOHC HadGEM3-GC31-LL model output prepared for CMIP6 ScenarioMIP ssp585. Version 20211003.Earth System Grid Federation. https://doi.org/10.22033/ESGF/CMIP6.10901, 2020.

Good, P., Sellar, A., Tang, Y., Rumbold, S., Ellis, R., Kelley, D., and Kuhlbrodt, T.: MOHC UKESM1.0-LL model output prepared for CMIP6 ScenarioMIP ssp585, Version 20211003, Earth System Grid Federation, https://doi.org/10.22033/ESGF/CMIP6.6405, 2019.

Heuzé, C.: Antarctic bottom water and North Atlantic deep water in CMIP6 models. Ocean Science, *17*(1), 59–90, https://doi.org/10.5194/ os-17-59-2021, 2021.

Holt, J, Hyder, P., Ashworth, M., Harle, J., Hewitt, H. T., Liu, H., New, A. L., Pickles, S., Porter,A., Popova, E., Allen, J. I., Siddorn, J., and Wood, R.: Prospects for imprroving the representation of coastal and shelf seas in global ocean models, Geosci. Model Dev., 10, 499-523, 2017.

Huang, W.: THU CIESM model output prepared for CMIP6 CMIP historical, Version 20211003, Earth System Grid Federation, https://doi.org/10.22033/ESGF/CMIP6.8843, 2019.

Huang, W.: THU CIESM model output prepared for CMIP6 ScenarioMIP ssp585, Version 20211003, Earth System Grid Federation, https://doi.org/10.22033/ESGF/CMIP6.8863, 2020.

Johns, W. E., Baringer, M. O., Beal, L. M., Cunningham, S. A., Kanzow, T., Bryden, H. L., Hirschi, J. Marotzke, J., Meinen, C., Shaw, B., and Curry, R.: Continuous, array-based estimates of Atlantic Ocean heat transport at 26.5°N, J. Clim., 24**,** 2429-2449, doi:10.1175/2010JCLI3997.1, 2011.

Johns, W.E., Elipot, S., Smeed, D. A., Moat, B., King, B., Volkov, D. L., and Smith, R. H.: Towards two decades of Atlantic Ocean mass and heat transports at 26.5 N, *Phil. Trans. R. Soc. A*, 381, https://doi.oorg/10.1098/rsta.2022.0188, 2023.

Jungclaus, J., Bittner, M., Wieners, K.-H., Wachsmann, F., Schupfner, M., Legutke, S., Giorgetta, M.; Reick, C., Gayler, V., Haak, H., de Vrese, P., Raddatz, T., Esch, M., Mauritsen, T., von Storch, J-S., Behrens, J., Brovkin, V., Claussen, M., Crueger, T., Fast, I., Fiedler, S., Hagemann, S., Hohenegger, C., Jahns, T., Kloster, S., Kinne, S., Lasslop, G., Kornblueh, L., Marotzke, J., Matei, D., Meraner, K., Mikolajewicz, U., Modali, K., Müller, W., Nabel, J., Notz, D., Peters-von Gehlen, K., Pincus, R., Pohlmann, H., Pongratz, J., Rast, S., Schmidt, H., Schnur, R., Schulzweida, U., Six, K., Stevens, B., Voigt, A., and Roeckner, E.: MPI-M MPI-ESM1.2-HR model output prepared for CMIP6 CMIP historical, Version 20211003, Earth System Grid Federation, https://doi.org/10.22033/ESGF/CMIP6.6594, 2019.

Lawrence, B. N.: Storing and manipulating environmental big data with JASMIN. in *2013 IEEE International Conference on Big Data* 68–75 (ieeexplore.ieee.org, 2013), doi:10.1109/BigData.2013.6691556.

Lee, J.-Y., J. Marotzke, J., Bala, G., Cao, L., Corti, S., Dunne, J.P., Engelbrecht, F., Fischer, E., Fyfe, J.C., Jones, C., Maycock, A.,Mutemi, J., Ndiaye, O., Panickal, S., and Zhou, T.: Future Global Climate: Scenario-Based Projections and Near- Term Information. In Climate Change 2021: The Physical Science Basis. Contribution of Working Group I to the Sixth Assessment Report of the Intergovernmental Panel on Climate Change [Masson-Delmotte, V., Zhai, P., Pirani, A., Connors, S.L. , Péan, C., Berger, S., Caud, N., Chen, Y., Goldfarb, L., Gomis, M. I., Huang, M., Leitzell, K., Lonnoy, E., Matthews, J. B. R., Maycock, T. K.; Waterfield, T., Yelekçi, O., Yu, R., and Zhou, B. (eds.)]. Cambridge University Press, Cambridge, United Kingdom and New York, NY, USA, pp. 553–672, doi:10.1017/9781009157896.006, 2021

Levang, S. J., and Schmitt, R. W.: What Causes the AMOC to Weaken in CMIP5? J. Clim., *33*(4), 1535-1545, 2020.

Li, G., Cheng, L., Zhu, J., Trenberth, K. E., Mann, M. E. and Abraham, J. P.: Increasing ocean stratification over the past half-century, Nat. Clim. Change 10, 1116–1123, 2020.

Lovato, T., and Peano, D.: CMCC CMCC-CM2-SR5 model output prepared for CMIP6, CMIP historical, Version 20211003,Earth System Grid Federation, https://doi.org/10.22033/ESGF/CMIP6.3825, 2020.

Lovato, T., and Peano, D.: CMCC CMCC-CM2-SR5 model output prepared for CMIP6, ScenarioMIP ssp585, Version 20211003, Earth System Grid Federation, https://doi.org/10.22033/ESGF/CMIP6.3896, 2020.

Lovato, T., Peano, D., and Butenschön, M.: CMCC CMCC-ESM2 model output prepared for CMIP6 CMIP historical, Version 20211003, Earth System Grid Federation. https://doi.org/10.22033/ESGF/CMIP6.13195, 2021.

Lovato, T., Peano, D., and Butenschön, M.: CMCC CMCC-ESM2 model output prepared for CMIP6 ScenarioMIP ssp585, Version 20211003, Earth System Grid Federation. https://doi.org/10.22033/ESGF/CMIP6.13259, 2021.

McCarthy, G. D., and Caesar, L.: Can we trust projections of AMOC weakening based on climate models that cannot reproduce the past?, Phil. Trans. Roy. Soc., 381(2262), https://doi.org/10.1098/rsta.2022.0193, 2023.

McCarthy, G. D., Smeed, D. A., Johns, W. E., Frajka-Williams, E., Moat, B. I., Rayner, D., Baringer, M. O., Meinen, C. S., and Bryden, H. L.: Measuring the Atlantic meridional overturning circulation at 26°N, Prog. Oceanogr., *130*, 91-111, doi:10.1016/j.pocean.2014.10.006, 2015..

Mecking, J.V. and Drijfhout, S. S.: The decrease in ocean heat transport in response to global warming, Nat. Clim. Change, 13. 1229-1236, https://doi.org/10.1038/s41558-023-01829-8, 2023.

Meinen, C. S., Johns, W. E., Moat, B. I., Smith, R. H., Johns, E. M., Rayner, D., Frajka-Williams, E., Garcia, R. F., and Garzoli, S. L.: Structure and variability of the Antilles Current at 26.5 N, *J. Geophys. Res. Oceans*, *124*, 3700-3723, doi:110.1029/2018JC014836, 2019.

Formatted: Font colour: Black

Formatted: Font colour: Black

Moat B. I., Smeed, D. A., Frajka-Williams, E., Desbruyeres, D. G., Beaulieu, C., Johns, W. E., Rayner, D., Sanchez-Franks, A., Baringer, M. O., Volkov, D., Jackson, L. C, and Bryden, H.L.: Pending recovery in the strength of the meridional overturning circulation at 26°N. Ocean Sci. 16, 863–874, doi:10.5194/os-16-863-2020, 2020.

Moat, B. I., Frajka-Williams, E., Smeed, D. A., Rayner, D., Johns, W. E., Baringer, M. O., Volkov, D. L., and Collins, J.: Atlantic meridional overturning circulation observed by the RAPID-MOCHA-WBTS (RAPID-meridional Overturning Circulation and Heatflux Array-Western Boundary Time Series) array at 26N from 2004 to 2020 (v2020.2). British Oceanographic Data Centre, Natural Environment Research Council [data set]. https://doi.org/10.5285/e91b10af-6f0a-7fa7-e053-6c86abc05a09, 2022.

Munk, W.: Abyssal recipes. Deep-Sea Res., 13, 707-730, 1966.

O'Neill, B. C., Tebaldi, C., Vuuren, D. P. V., Eyring, V., Friedlingstein, P., Hurtt, G., Knutti, R., Kriegier, E., Lamarque, J.-F., Lowe, J., Meehl, G. A., Moss, R., Riiahi, K., and Sanderson, B. M.: The scenario model intercomparison project (ScenarioMIP) for CMIP6, Geoscientific Model Development, 9(9), 3461–3482 https://doi.org/10.5194/gmd-9-3461-2016, 2016.

Piecuch, C. G., and Beal, L. M.: Robust Weakening of the Gulf Stream During the Past Four Decades Observed in the Florida Straits, Geophys. Res. Lett., 50, https://doi.org:10.1029/2023gl105170, 2023.

Ridley, J., Menary, M., Kuhlbrodt, T., Andrews, M., and Andrews, T.: MOHCHadGEM3-GC31-LL model output prepared for CMIP6 CMIP historical, Version 20211003, Earth System Grid Federation, https://doi.org/10.22033/ESGF/CMIP6.6109, 2019.

Ridley, J., Menary, M., Kuhlbrodt, T., Andrews, M., Andrews, T.: MOHCHadGEM3-GC31-MM model output prepared for CMIP6 CMIP historical, Version 20211003, Earth System Grid Federation, https://doi.org/10.22033/ESGF/CMIP6.6112, 2019.

Roberts, M. J., Jackson, L. C., Roberts, C. D., Meccia, V., Docquier, D., Koenigk, T.,Ortega, P., Moreno-Chamarro, E., Bellucci, A., Coward, A., Drijfhout, S., Exarchou, E., Gutjahr, O., Hewitt, H., Iovino, D., Lohmann, K., Putrasahan, D., Schiemann, R., Seddon, J., Terray, L., Xu, X., Zhang, Q., Chang, P., Yeager, S. G., Castruccio, F. S., Zhang, S., and Wu, L.: Sensitivity of the Atlantic meridional overturning circulation to model resolution in CMIP6 HighResMIP simulations and implications for future changes, J. Adv. Modeling Earth Sys, *12*(8), e2019MS002014, 2020.

Rong, X.: CAMS CAMS_CSM1.0 model output prepared for CMIP6 CMIP historical, Version 20211003, Earth System Grid Federation. https://doi.org/10.22033/ESGF/CMIP6.9754, 2019.

Rong, X.: CAMS CAMS-CSM1.0 model output prepared for CMIP6 ScenarioMIP ssp585, Version 20211003, Earth System Grid Federation, https://doi.org/10.22033/ESGF/CMIP6.11052, 2019.

Schupfner, M., Wieners, K.-H., Wachsmann, F., Steger, C., Bittner, M., Jungclaus, J., Früh, B., Pankatz, K., Giorgetta, M., Reick, C., Legutke, S., Esch, M., Gayler, V., Haak, H., de Vrese, P., Raddatz, T., Mauritsen, T., von Storch, J.-S., Behrens, J., Brovkin, V., Claussen, M., Crueger, T., Faust, I., Fiedler, S., Hagemann, S., Hohenegger, C., Jahns, T., Kloster, S., Kinne, S., Lasslop, G., Kornblueh, L., Marotzke, J., Matei, D., Meraner, K., Mikolajewicz, U., Modali, K., Müller, W., Nabel, J., Notz, D., Peters-von Gehlen, K., Pincus, R., Pohlmann, H., Pongratz, J., Rast, S., Schmidt, H., Schnur, R., Schulzweida, U., Six, K., Stevens, B., Voigt, A., and Roeckner, E.: DKRZ MPI-ESM1.2-HR model output prepared for CMIP6 ScenarioMIPssp585, Version 20211003, Earth System Grid Federation. https://doi.org/10.22033/ESGF/CMIP6.4403, 2019.

Seferian, R.: CNRM-CERFACS CNRM-ESM2-1 model output prepared for CMIP6 CMIP Historical, Version 20211003, Earth System Grid Federation. https://doi.org/10.22033/ESGF/CMIP6.4068, 2018.

Smeed, D. A., Josey, S. A., Beaulieu, C., Johns, W.E., Moat, B. I., Frajka-Williams, E., Rayner, D., Meinen, C. S., Baringer, M. O., Bryden, H. L., and McCarthy, G. D.: The North Atlantic Ocean is in a state of reduced overturning, Geophys. Res. Lett., 45, https://doi.org/10.1002/2017GL076350, 2018.

Song, Z., Qiao, F., Bao, Y., Shu, Q., Song, Y., and Yang, X.: FIO-QLNM FIO-ESM2.0 model output prepared for CMIP6 CMIP historical. Version 20211003.Earth System Grid Federation. https://doi.org/10.22033/ESGF/CMIP6.9199, 2019.

Song, Z., Qiao, F., Bao, Y., Shu, Q., Song, Y., and Yang, X.: FIO-QLNM FIO-ESM2.0 model output prepared for CMIP6 ScenarioMIP ssp585, Version 20211003, Earth System Grid Federation. https://doi.org/10.22033/ESGF/CMIP6.9214, 2019.

Stommel, H.: The westward intensification of wind-driven ocean currents. Eos, Trans. American Geophys. Union, *29*(2), 202-206, 1948.

Swart, N. C., Cole, J. N. S., Kharin, V. V., Lazare, M., Scinocca, J. F., Gillett, N. P., Anstey, J., Arora, V., Christian, J. R., Jiao, Y., Lee, W. G., Majaess, F., Saenko, O. A., Seiler, C., Seinen, C., Shao, A., Solheim, L., von Salzen, K., Yang, D., Winter, B., and Sigmond, M: CCCma CanESM5 model output prepared for CMIP6 CMIP historical, Version 20211003, Earth System Grid Federation, https://doi.org/10.22033/ESGF/CMIP6.3610, 2019.

Swart, N. C., Cole, J. N. S., Kharin, V. V., Lazare, M., Scinocca, J. F., Gillett, N. P., Anstey, J., Arora, V., Christian, J. R., Jiao, Y., Lee, W. G., Majaess, F., Saenko, O. A., Seiler, C., Seinen, C., Shao, A., Solheim, L., von Salzen, K., Yang, D., Winter, B., and Sigmond, M.: CCCma CanESM5 model output prepared for CMIP6 ScenarioMIP ssp585, Version 20211003, Earth System Grid Federation. https://doi.org/10.22033/ESGF/CMIP6.3696, 2019.

Tang, Y., Rumbold, S., Ellis, R., Kelley, D., Mulcahy, J., Sellar, A., Walton, J., and Jones, C.: MOHC UKESM1.0-LL model output prepared for CMIP6 CMIP Historical, Version 20211003 Earth System Grid Federation, https://doi.org/10.22033/ESGF/CMIP6.6113, 2019.

Toggweiler, J. R., and Samuels, B.: On the ocean's large-scale circulation near the limit of no vertical mixing, J. Phys. Oceanogr, *28*(9), 1832–1852. https://doi.org/10.1175/1520-0485(1998)028, 1998.

Voldoire, A.: CNRM-CERFACS CNRM-CM6-1-HR model output prepared for CMIP6 CMIP Historical, Version 20211003, Earth System Grid Federation, https://doi.org/10.22033/ESGF/CMIP6.4067, 2019.

Voldoire, A.: CNRM-CERFACS CNRM-CM6-1-HR model output prepared for CMIP6 ScenarioMIP ssp585, Version 20211003, Earth System Grid Federation. https://doi.org/10.22033/ESGF/CMIP6.4225, 2019.

Weijer, W., Cheng, W., Garuba, O. A., Hu, A., and Nadiga, B. T.: CMIP6 models predict significant 21st century decline of the Atlantic Meridional Overturning Circulation, Geophys. Res. Lett., *47*(12), doi:10.10029/2019GL086075, 2020.

Formatted: Font: Not Italic

Formatted: Font: Italic

Wieners, K.-H., Giorgetta, M., Jungclaus, J., Reick, C., Esch, M., Bittner, M., Legutke, S., Schupfner, M., Wachsmann, F., Gayler, V., Haak, H., de Vrese, P., Raddatz, T., Mauritsen, T., von Storch, J.-S., Behrens, J., Brovkin, V., Claussen, M., Crueger, T., Fast, I., Fiedler, S., Hagemann, S., Hohenegger, C., Jahns, T., Kloster, S., Kinne, S., Lasslop, G., Kornblueh, L., Marotzke, J., Matei, D., Meraner, K., Mikolajewicz, U., Modali, K., Müller, W., Nabel, J., Notz, D., Peters-von Gehlen, K., Pincus, R., Pohlmann, H., Pongratz, J., Rast, S., Schmidt, H.; Schnur, R., Schulzweida, U., Six, K., Stevens, B., Voigt, A., and Roeckner, E.: MPI-M MPI-ESM1.2-LR model output prepared for CMIP6 CMIP historical, Version 20211003, Earth System Grid Federation, https://doi.org/10.22033/ESGF/CMIP6.6595, 2019.

Wieners, K.-H., Giorgetta, M., Jungclaus, J., Reick, C., Esch, M., Bittner, M., Gayler, V., Haak, H., de Vrese, P., Raddatz, T., Mauritsen, T., von Storch, J.-S., Behrens, J., Brovkin, V., Claussen, M., Crueger, T., Fast, I., Fiedler, S., Hagemann, S., Hohenegger, C., Jahns, T., Kloster, S., Kinne, S., Lasslop, G., Kornblueh, L., Marotzke, J., Matei, D., Meraner, K., Mikolajewicz, U., Modali, K., Müller, W., Nabel, J., Notz, D., Peters-von Gehlen, K., Pincus, R., Pohlmann, H., Pongratz, J., Rast, S., Schmidt, H., Schnur, R., Schulzweida, U., Six, K., Stevens, B., Voigt, A., and Roeckner, E.: MPI-M MPI-ESM1.2-LR model output prepared for CMIP6 ScenarioMIP ssp585, Version 20211003, Earth System Grid Federation, https://doi.org/10.22033/ESGF/CMIP6.6705, 2019.

Yan, X., Zhang, R., and Knutson, T. R.: Underestimated AMOC variability and implications for AMV and predictability in CMIP models, Geophys. Res. Lett., *45*(9), 4319-4328, 2018.

Yukimoto, S., Koshiro, T., Kawai, H., Oshima, N., Yoshida, K., Urakawa, S., Tsujino, H., Deushi, M., Tanaka, T., Hosaka, M., Yoshimura, H., Shindo, E., Mizuta, R., Ishii, M., Obata, A., and Adachi, Y.: MRI MRI-ESM2.0 model output prepared for CMIP6 CMIP historical, Version 20211003, Earth System Grid Federation, https://doi.org/10.22033/ESGF/CMIP6.6842, 2019.

Yukimoto, S., Koshiro, T., Kawai, H., Oshima, N., Yoshida, K., Urakawa, S., Tsujino, H., Deushi, M., Tanaka, T., Hosaka, M., Yoshimura, H., Shindo, E., Mizuta, R., Ishii, M., Obata, A., and Adachi, Y.: MRI MRI-ESM2.0 model output prepared for CMIP6 ScenarioMIP ssp585, Version 20211003, Earth System Grid Federation, https://doi.org/10.22033/ESGF/CMIP6.6929, 2019.

Zhao, J., and Johns, W.: Wind-forced interannual variability of the Atlantic Meridional Overturning Circulation at 26.5 N, J. Geophys. Res. Oceans, 119, 2403-2419, doi:10.1002/2013JC009407, 2014.

Formatted: No widow/orphan control, Don't adjust space between Latin and Asian text, Don't adjust space between Asian text and numbers, Tab stops: 0.99 cm, Left + 1.98 cm, Left + 2.96 cm, Left + 3.95 cm, Left + 4.94 cm, Left + 5.93 cm, Left + 6.91 cm, Left + 7.9 cm, Left + 8.89 cm, Left + 9.88 cm, Left + 10.86 cm, Left + 11.85 cm, Left

Page 10: [1] Deleted Harry Bryden 24/01/2024 14:55:00